AD-A194 560 PHOTOREFRACTIVE DAMAGE MECHANISM IN ELECTRO-OPTIC MATERIALS(U) OKLAHOMA STATE UNIV STILLWATER DEPT OF PHYSICS L E HALLIBURTON 01 MAR 88 AFOSR-TR-88-0451 1/1

UNCLASSIFIED AFOSR-85-0270 F/G 20/5 NL

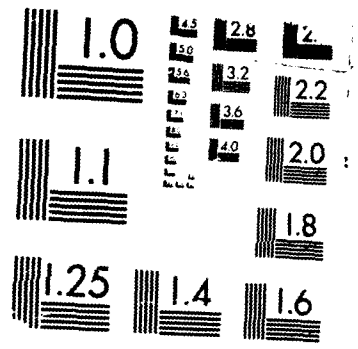

(2)

REPORT DOCUMENTATION PAGE

DTIC ELECTE MAY 0 3 1988 D

AD-A194 560

1a. REPORT SECURITY CLASSIFICATION: Unclassified	1b. RESTRICTIVE MARKINGS
2a. SECURITY CLASSIFICATION AUTHORITY	3. DISTRIBUTION/AVAILABILITY OF REPORT: Distribution unlimited
2b. DECLASSIFICATION/DOWNGRADING SCHEDULE	
4. PERFORMING ORGANIZATION REPORT NUMBER(S)	5. MONITORING ORGANIZATION REPORT NUMBER(S): AFOSR-TR- 88-0451
6a. NAME OF PERFORMING ORGANIZATION: Oklahoma State University	6b. OFFICE SYMBOL (If applicable):
6c. ADDRESS (City, State and ZIP Code): Department of Physics, Stillwater, OK 74078	7b. ADDRESS (City, State and ZIP Code): Building 410, Bolling AFB, DC 20332-6448
8a. NAME OF FUNDING/SPONSORING ORGANIZATION: AFOSR	8b. OFFICE SYMBOL (If applicable): NE
8c. ADDRESS (City, State and ZIP Code): Building 410, Bolling AFB, DC	9. PROCUREMENT INSTRUMENT IDENTIFICATION NUMBER: AFOSR-85-0270
	10. SOURCE OF FUNDING NOS. — PROGRAM ELEMENT NO.: 61102F; PROJECT NO: 2305; TASK NO.: B1; WORK UNIT NO:
11. TITLE (Include Security Classification): Photorefractive Damage Mechanism in Electro-Optic Materials	
12. PERSONAL AUTHOR(S): Larry E. Halliburton	
13a. TYPE OF REPORT: annual	13b. TIME COVERED: FROM 7-15-87 TO 2-15-88
14. DATE OF REPORT (Yr., Mo., Day): March 1, 1988	15. PAGE COUNT: Printed Pages
16. SUPPLEMENTARY NOTATION	
17. COSATI CODES — FIELD / GROUP / SUB GR.	18. SUBJECT TERMS (Continue on reverse if necessary and identify by block number)

19. ABSTRACT (Continue on reverse if necessary and identify by block number)

The photo-induced redistribution of charge has been characterized in $Bi_{12}GeO_{20}$ and $Bi_{12}SiO_{20}$ crystals using electron spin resonance, thermally stimulated luminescence, and optical absorption techniques. Our results suggest that Fe^{3+} ions play an important role in the photorefractive effect in these materials.

(Keywords: Bismuth compounds, Silicon compounds, Germanium compounds)

20. DISTRIBUTION/AVAILABILITY OF ABSTRACT: UNCLASSIFIED/UNLIMITED ☐ SAME AS RPT. ☐ DTIC USERS ☐	21. ABSTRACT SECURITY CLASSIFICATION: Unclass
22a. NAME OF RESPONSIBLE INDIVIDUAL: Giles	22b. TELEPHONE NUMBER (Include Area Code): 202-767-4933 — 22c. OFFICE SYMBOL: NE

DD FORM 1473, 83 APR — EDITION OF 1 JAN 73 IS OBSOLETE.

SECURITY CLASSIFICATION OF THIS PAGE

SUMMARY OF PROGRESS

In the present reporting period, we have concentrated on measurements of the light-induced migration of charge in photorefractive $Bi_{12}SiO_{20}$ and $Bi_{12}GeO_{20}$ crystals. Specifically, the photo-induced redistribution of charge has been characterized in $Bi_{12}GeO_{20}$ and $Bi_{12}SiO_{20}$ crystals using electron spin resonance, thermally stimulated luminescence, and optical absorption techniques. Excitation with 350-nm light at 77 K converts Fe^{3+} ions to Fe^{2+} ions. The source of electrons (i.e., the hole traps) is not known, but they may be other impurities or intrinsic defects such as vacancies or anti-site cations. As the crystals are warmed to room temperature, recovery of the Fe^{3+} ions correlates with thermoluminescence peaks at 145, 165, and 245 K. We postulate that Fe^{2+} ions are the recombination site and that each thermoluminescence peak corresponds to the release of holes from a different trap. Our results suggest that Fe^{3+} ions may play an important role in the photorefractive effect in these materials.

The results contained in this report have been prepared for submission to the Journal of Applied Physics.

I. INTRODUCTION

Photorefractive materials such as $LiNbO_3$, $BaTiO_3$, $Bi_{12}SiO_{20}$, and $Bi_{12}GeO_{20}$ are being extensively studied at the present time because of their potential applications in optical data processing.[1-4] When these crystals are exposed to interfering laser beams, electrons are released from impurity ions in the bright fringe regions. These electrons then move to the adjacent dark fringe regions where they become retrapped. The redistribution of charge resulting from these photoexcitation and retrapping processes creates an added component to the crystal's internal electric field which, in turn, changes the refractive index of the material via the electro-optic effect. The spatial variation of this added internal electric field corresponds to the interference pattern produced by the initial laser beams.

Early models of the photorefractive effect were based on the assumption that only one type of charge carrier (either holes or electrons) was participating in the charge migration process.[5-6] However, investigators[7-9] have had to consider the transport of both types of carriers in order to explain their results in materials such as $LiNbO_3$ and $BaTiO_3$. In contrast, photoconductivity results[10,11] from $Bi_{12}SiO_{20}$ and $Bi_{12}GeO_{20}$ indicate that the contribution from electrons is at least an order of magnitude greater than that from holes. This led to the generally accepted notion that only electrons needed to be considered when explaining the photorefractive effect in these latter materials. More recently, Strohkendl and Hellwarth[12] have provided evidence that the one-charge-carrier model is not entirely applicable even in

the case of $Bi_{12}SiO_{20}$.

Identifying the specific impurities and other defects which participate in the photorefractive effect is an important goal since this information will allow a material to be optimized for a particular set of applications. In the present report, we describe using spectroscopic techniques such as electron spin resonance (ESR), thermally stimulated luminescence (TSL), and optical absorption to characterize point defects in commercially grown, undoped crystals of $Bi_{12}GeO_{20}$ and $Bi_{12}SiO_{20}$ (hereafter referred to as BGO and BSO, respectively). Much of our attention has been focused on the behavior of Fe^{3+} impurity ions after photoexcitation at 77 K. Correlations are found in the ESR and TSL data.

II. EXPERIMENTAL PROCEDURE

The BGO crystals were purchased from Crystal Technology, Palo Alto, CA and the BSO crystals were provided by Union Carbide, Washougal, WA. Samples for the ESR experiments were cut from the larger crystals and had dimensions of 2 x 3 x 8 mm^3. Optical samples for the absorption and the TSL experiments had dimensions of 2 x 10 x 15 mm^3. The two broad faces of the optical samples were polished.

An IBM Instruments (Bruker) Model ER200D spectrometer was used to obtain the ESR data. It operated at X-band (9.3 GHz) with a modulation frequency of 100 kHz. The magnetic field and the microwave frequency were measured with a Varian E-500 gauss-

meter and a Hewlett Packard 5340A counter, respectively. A small quartz-tipped finger Dewar extending into the microwave cavity allowed the ESR sample to be immersed directly in liquid nitrogen during the measurements.

Optical absorption spectra were taken with a Perkin-Elmer Model 330 dual-beam spectrophotometer. In these measurements, the sample was mounted on a copper cold-finger which extended below the liquid nitrogen reservoir of a home-built metal Dewar. This allowed the sample's temperature to be maintained at approximately 80 K. The same optical Dewar was used to collect the TSL data. In these experiments, the emitted light was detected with an RCA 7102 photomultiplier tube placed immediately adjacent to the Dewar window and in front of the broad face of the sample. This particular phototube was chosen because of its greater sensitivity in the near infrared spectral region. A Keithley 600B electrometer converted the output of the phototube into a signal suitable for recording. No attempt was made to use a monochromator or filters to selectively examine the emission in the various regions of the optical spectrum.

A 150-W mercury-xenon lamp and a 25-cm monochromator (SPEX Minimate) set at 350 nm with a 5-mm exit slit was used to induce the charge redistributions in the ESR and optical experiments.

III. EXPERIMENTAL RESULTS

A. Electron spin resonance

Although our BGO and BSO samples were not deliberately doped with transition-metal ions, we expected that trace amounts of

these impurities (at the level of a few ppm) might appear in our initial ESR spectra. Somewhat to our surprise, we discovered that a single, rather intense ESR spectrum representing a concentration of approximately 5 x 10^{19} impurity ions per cm^3 was present in the as-grown BGO samples. This spectrum is shown in Fig. 1(a). A nearly identical ESR spectrum at a similar concentration was found in the as-grown BSO samples. Wardzynski et al.[13] have assigned this spectrum in BGO to Fe^{3+} ions substituting for Ge^{4+} ions and von Bardeleben[14] has assigned the equivalent spectrum in BSO to Fe^{3+} ions substituting for Si^{4+} ions. Both investigators concluded that the necessary charge compensation was nonlocal. The Fe^{3+} ESR spectrum shown in Fig. 1(a) was taken at 77 K with the magnetic field parallel to the [100] direction. It appears to be three equally spaced lines; however, the five lines required for an $S = 5/2$ ($3d^5$) spin system are present in Fig. 1(a) since each of the two outer lines represents two unresolved transitions. This set of five lines collapses into one line when the magnetic field is rotated approximately 30° from the [100] direction in the (001) plane.

When the BGO sample is exposed to 350-nm light at 77 K for 5 min, a significant reduction in the Fe^{3+} ESR spectrum occurs. This effect is illustrated in Fig. 1(b). Since another ESR spectrum does not appear, we are unable to specify the new charge state of the Fe ions. Both Fe^{2+} and Fe^{4+} states are possible, but we favor Fe^{2+} because of the accompanying optical absorption spectrum (see Section III-C) and also because Mn^{2+} ions have been reported[15] to occupy the tetrahedral sites in BGO and BSO.

As long as the sample is maintained at 77 K, the new charge state of the Fe ions is stable; however, returning the sample to room temperature restores the Fe^{3+} ESR spectrum to its original size. To further characterize this recovery process, a pulsed thermal anneal experiment was performed. First, the sample was exposed to 350-nm light for 5 min at 77 K and the intensity of the residual Fe^{3+} signal was measured. Next, the sample was subjected to a series of four-minute anneals at progressively higher temperatures between 77 and 300 K. After each anneal, the sample was returned to 77 K where the intensity of the Fe^{3+} ESR signal was monitored. The dashed curve in Fig. 2 illustrates the thermal recovery of the Fe^{3+} spectrum in BGO after its near elimination by the UV light at low temperature. Half of the Fe^{3+} ions have returned by 165 K and nearly all of them have returned by 200 K.

Photo-excitation of the BSO samples with 350-nm light at 77 K also destroyed more than 95% of the original Fe^{3+} ESR spectrum. The recovery of this signal during a subsequent thermal anneal is illustrated by the dashed curve in Fig. 3. In contrast to the results from BGO, the Fe^{3+} ESR spectrum recovers in two steps, one between 125 and 200 K and the other near 245 K.

B. Thermally stimulated luminescence

Earlier investigators[16,17] have reported a series of TSL peaks below room temperature in both BGO and BSO. Excitation with ultraviolet light at low temperature gave rise to prominent TSL peaks near 160 and 240 K with the maximum in the emission spectrum occurring in the infrared at about 1.3 eV. With only

TSL data, these scientists could not identify any of the responsible defects. As a result of having access to both ESR and TSL instrumentation in the present investigation, we have been able to establish that Fe^{3+} ions are participants in the TSL process in these two materials.

The solid curve in Fig. 2 shows the TSL data from our BGO sample. The crystal was first exposed to 350-nm light for five min at 80 K to redistribute the charge, then the temperature was increased at a linear rate while the emitted light was monitored. A small cartridge heater in the bottom of the empty liquid nitrogen reservoir of the optical Dewar provided the thermal energy. The heating rate was approximately 9 K/min from 80 K to 300 K. An intense peak near 165 K with a shoulder at 145 K is present along with another small peak at 240 K. These TSL results are in agreement with those previously reported by Lauer.[16] From a comparison of the ESR and TSL data in Fig. 2, we conclude that the recovery of the Fe^{3+} ESR signal correlates with the 165-K TSL peak in BGO.

The TSL data from our BSO sample is represented by the solid curve in Fig. 3. The same three peaks, at 145, 165, and 245 K, which were found in BGO are also present in BSO. However, the intensities of the peaks at 145 K and 245 K are considerably greater in BSO than in BGO. We assume that the different intensities for the peaks in the two samples is simply a result of different concentrations of either trapping or recombination sites. As shown in Fig. 3, the Fe^{3+} ESR spectrum in BSO recovers in two steps after the 77-K optical bleach. The first recovery

step between 125 K and 200 K correlates with the combined 145- and 165-K TSL peaks and the second Fe^{3+} recovery step closely parallels the 245-K TSL peak.

C. Optical absorption

In addition to the ESR and TSL studies, we also investigated the effect that an 80-K optical bleach would have on the optical absorption spectra of the BGO and BSO samples. The lower curve in Fig. 4 is the absorption spectrum, taken at 80 K, of an as-grown BGO sample. According to Hou et al.,[10] the band edge is near 3.4 eV at 80 K. Thus, the additional absorption extending out from the band edge in the 2.5 to 3.4 eV region must come from the unresolved "shoulder" initially reported by Hou et al.[10] and subsequently studied by numerous groups.[18-20] The origin of this absorption shoulder is still a subject of considerable controversy. Germanium or silicon vacancy complexes have been suggested by some to be the responsible defects, while others have proposed bismuth substituting for germanium or silicon.

Illuminating the BGO sample for five min at 80 K with 350-nm light induced a broad absorption extending across the entire visible region of the spectrum, as shown by the upper curve in Fig. 4. The difference between the two absorption spectra (i.e., as-received and after the 80-K optical bleach) is plotted in the inset. It consists of an absorption band peaking at 2.6 eV (477 nm) along with a shoulder on the low-energy side. A similar absorption spectrum was induced in BSO with 350-nm light. In $LiNbO_3$, Fe^{2+} ions are responsible for a broad absorption band peaking near 500 nm and, by analogy, we suggest that the 2.6-eV

band in BGO and BSO is due to Fe^{2+} ions. The obvious and immediate result of this photo-induced absorption spectrum is to make the BGO and BSO samples appear black to the human eye.

The thermal stability of the 2.6-eV absorption band was determined in the case of BGO. After being exposed to 350-nm light for 5 min at 80 K, the crystal was subjected to the same sequence of annealing steps as the earlier ESR samples. It was heated to a specified temperature, held there for 4 minutes, then recooled to 80 K where the optical absorption was measured. This procedure was then repeated at the next higher anneal temperature. Although the results are not shown, we found that the photo-induced absorption decays over the range from 125 to 200 K. This correlates well with the recovery of the Fe^{3+} ESR spectrum and the TSL peaks in BGO.

IV. CONCLUSIONS

Excitation of BGO and BSO crystals at low temperature with 350-nm light converts Fe^{3+} ions to Fe^{2+} ions. The source of these electrons is not known, but among the possibilities are undetected transition-metal-ion impurities, neutral oxygen vacancies, germanium or silicon vacancy complexes, and anti-site bismuth ions. Warming the samples to room temperature results in a series of TSL peaks when these photo-induced electron and hole pairs recombine. Since the infrared emission spectrum is the same for all of the TSL peaks,[16] we postulate that the recombination process is initiated by the release of holes from three

distinct trapping sites. One of these traps thermally releases holes at 145 K, another at 165 K, and the last at 245 K. The participation of Fe^{2+} ions in the 245-K TSL peak precludes the possibility that the release of electrons from Fe^{2+} ions initiates the recombination process at 145 K and 165 K.

A final observation relates to the defects responsible for the photorefractive effect in BGO and BSO. From the present work and other reports,[14,15,21] it appears that all BGO and BSO crystals, even undoped, contain significant amounts of Fe^{3+} ions which can easily change valence state upon illumination. At room temperature, these changes would be transitory and could account for the observed lifetimes of laser-induced gratings.[22,23] Thus, we suggest that Fe^{3+} impurity ions play a critical role in the photorefractive effect in BGO and BSO.

REFERENCES

1. A. M. Glass, Opt. Engineering 17, 471 (1978).
2. P. Gunther, Phys. Rep. 93, 199 (1982).
3. M. B. Klein and R. N. Schwartz, J. Opt. Soc. Am. B 3, 293 (1986).
4. F. Vachss and L. Hesselink, J. Opt. Soc. Am. B 4, 325 (1987).
5. N. V. Kukhtarev, Sov. Tech. Phys. Lett. 2, 438 (1976).
6. N. V. Kukhtarev, V. B. Markov, S. G. Odulov, M. S. Soskin, and V. L. Vinestkii, Ferroelectrics 22, 949 (1979).
7. R. Orlowski and E. Kratzig, Solid State Commun. 27, 1351 (1978).
8. M. B. Klein and G. C. Valley, J. Appl. Phys. 57, 4901 (1985).
9. S. Ducharme and J. Feinberg, J. Opt. Soc. Am. B 3, 283 (1986).
10. S. L. Hou, R. B. Lauer, and R. E. Aldrich, J. Appl. Phys. 44, 2652 (1973).
11. B. Kh. Kostyuk, A. Yu. Kudzin, and G. Kh. Sokolyanskii, Sov. Phys. Solid State 22, 1429 (1980).
12. F. P. Strohkendl and Hellwarth, J. Appl. Phys. 62, 2450 (1987).
13. W. Wardzynski, M. Baran, and H. Szymczak, Physica 111B, 47 (1981).
14. H. J. von Bardeleben, J. Phys. D: Appl. Phys. 16, 29 (1983).
15. W. Wardzynski, H. Szymczak, M. T. Borowiec, K. Pataj, T. Lukasiewicz, and J. Zmija, J. Phys. Chem. Solids 46, 1117 (1985).
16. R. B. Lauer, J. Appl. Phys. 42, 2147 (1971).

17. B. W. Holmes, J. E. Ludman, and C. L. Woods, in Basic Properties of Optical Materials: Summaries of Papers, 1985, Nat'l Bur. of Standards Special Publication 697, edited by A. Feldman, pp. 242-245; see also B. W. Holmes, E. Hammond, and S. Weathersby, Bull. Am. Phys. Soc. 31, 696 (1986).
18. O. A. Gudaev, V. A. Detinenko, and V. K. Malinovskii, Sov. Phys. Solid State 23, 109 (1981).
19. R. Oberschmid, Phys. Stat. Sol. (a) 89, 263 (1985).
20. B. C. Grabmaier and R. Oberschmid, Phys. Stat. Sol. (a) 96, 199 (1986).
21. W. Wardzynski, H. Szymczak, K. Pataj, T. Lukasiewicz, and J. Zmija, J. Phys. Chem. Solids 43, 767 (1982).
22. R. A. Mullen and R. W. Hellwarth, J. Appl. Phys. 58, 40 (1985).
23. L. Arizmendi and R. C. Powell, J. Appl. Phys. 62, 896 (1987).

FIGURE CAPTIONS

Fig. 1. The ESR spectrum of Fe^{3+} ions in BGO taken at 77 K with the magnetic field parallel to the [100] direction. Trace (a) was before and trace (b) was after a 5-min exposure to 350-nm light. The spectrometer gain was the same for both spectra.

Fig. 2. Thermal recovery of the Fe^{3+} ESR spectrum (dashed curve) and TSL peaks (solid curve) after low-temperature photo-excitation of BGO.

Fig. 3. Thermal recovery of the Fe^{3+} ESR spectrum (dashed curve) and TSL peaks (solid curve) after low-temperature photo-excitation of BSO.

Fig. 4. Effect of UV light on the optical absorption spectra of BGO. The lower trace was taken before and the upper trace after a 5-min exposure to 350-nm light at 80 K. The photo-induced absorption band (i.e., the difference between these two traces) is shown in the inset.

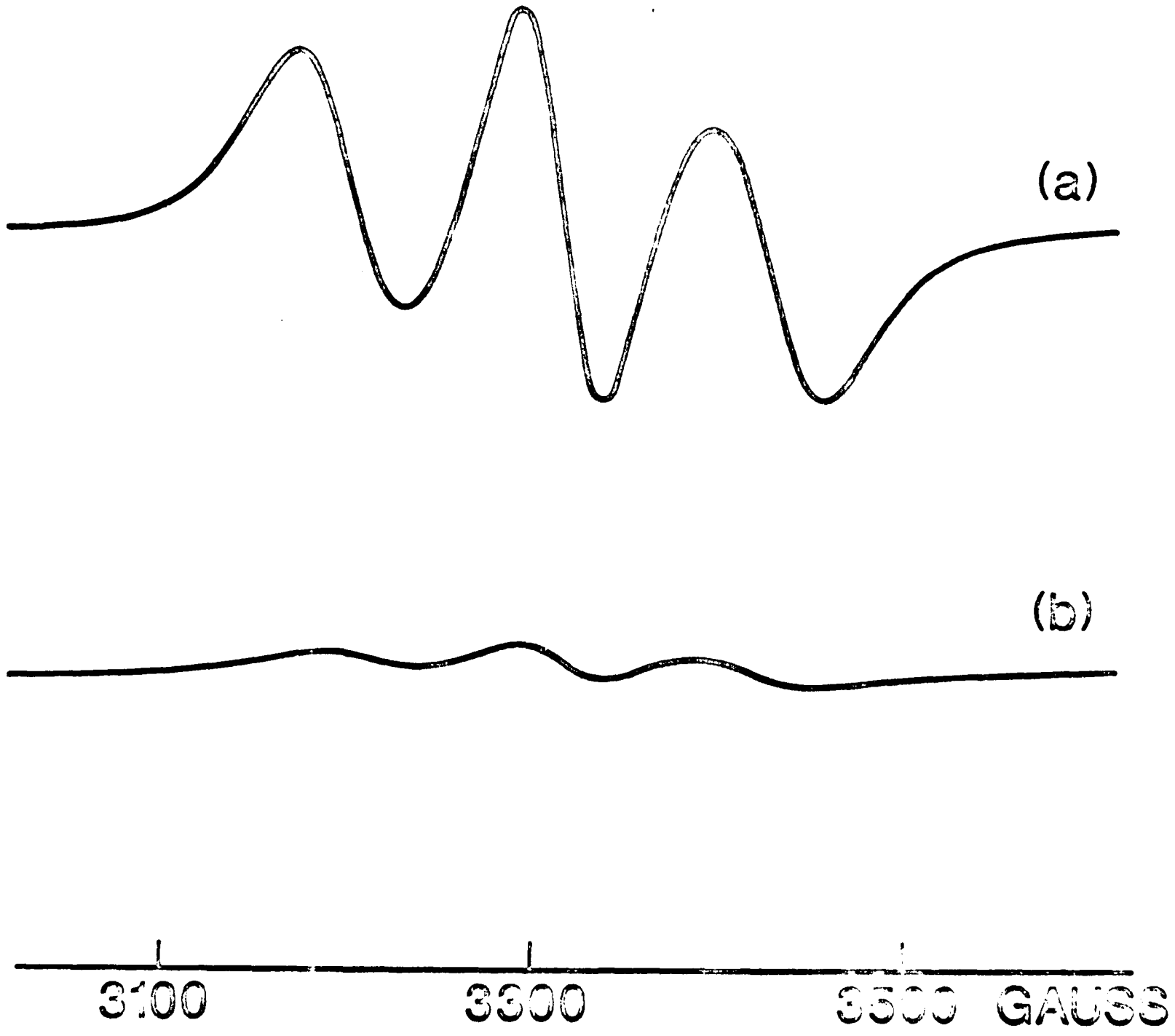
(a)
(b)
3100
3300
GAUSS

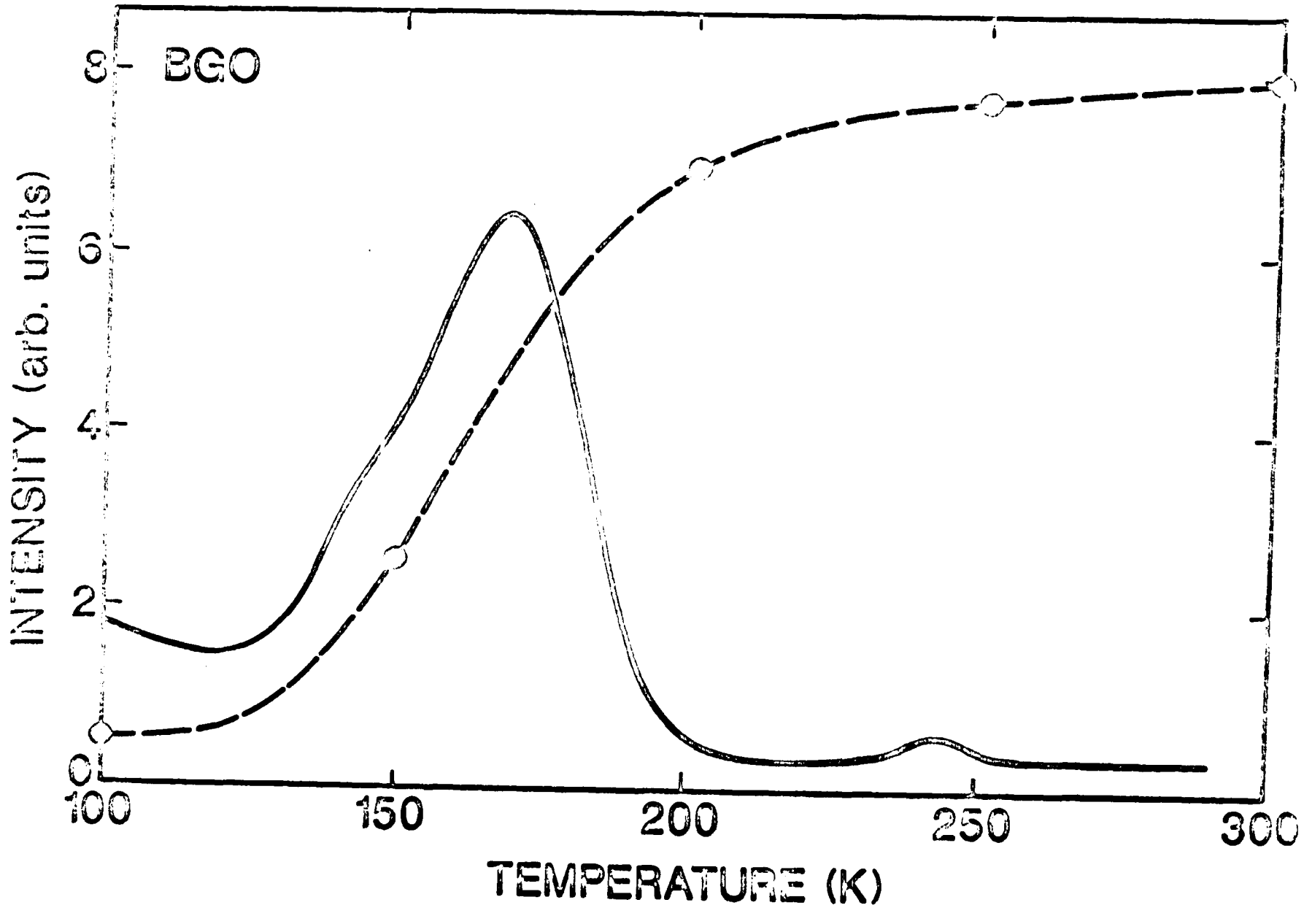
BGO
INTENSITY (arb. units)
0
2
4
6
8
100
150
200
250
300
TEMPERATURE (K)

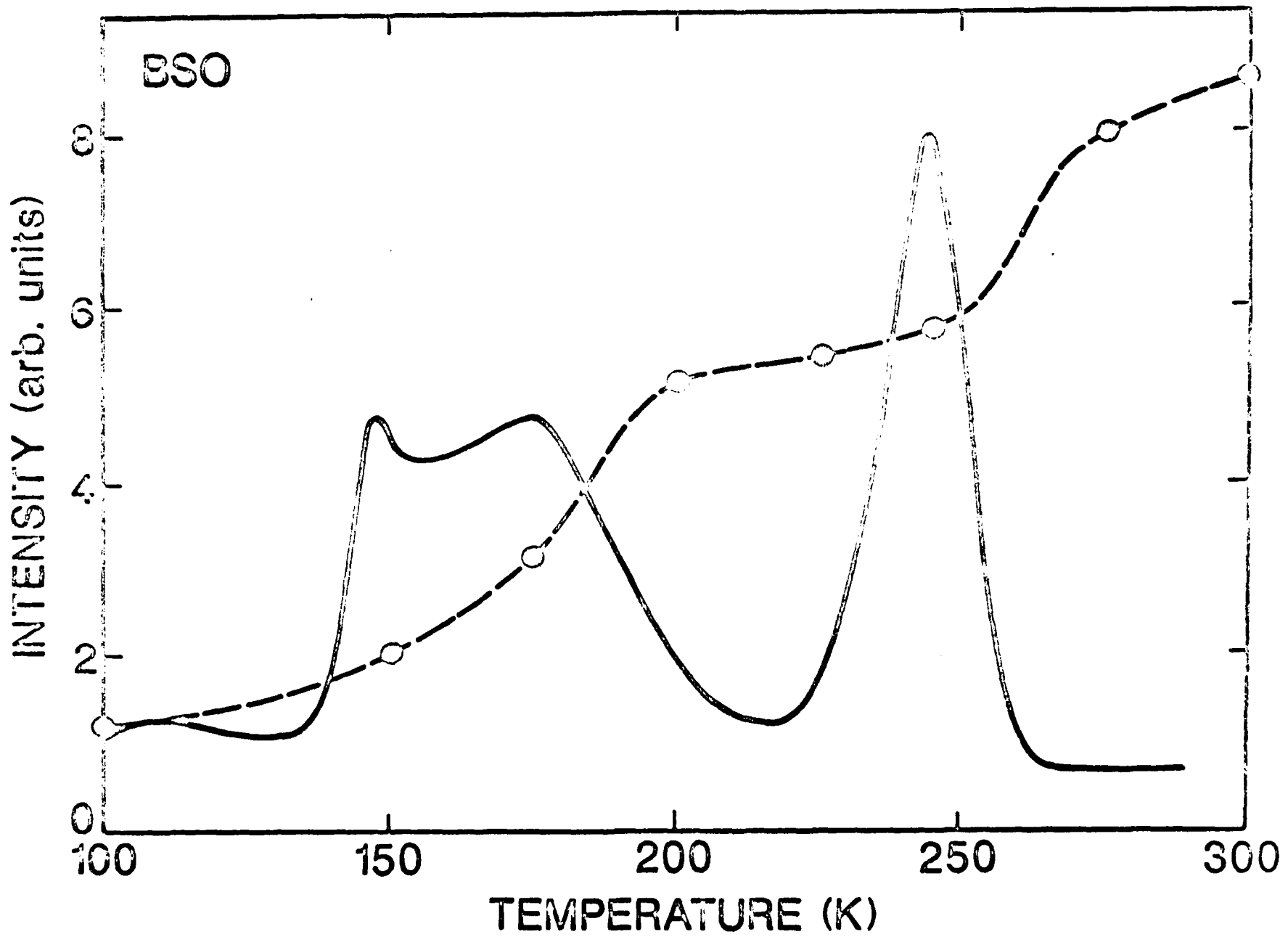
BSO
INTENSITY (arb. units)
0
2
4
6
8
100
150
200
250
300
TEMPERATURE (K)

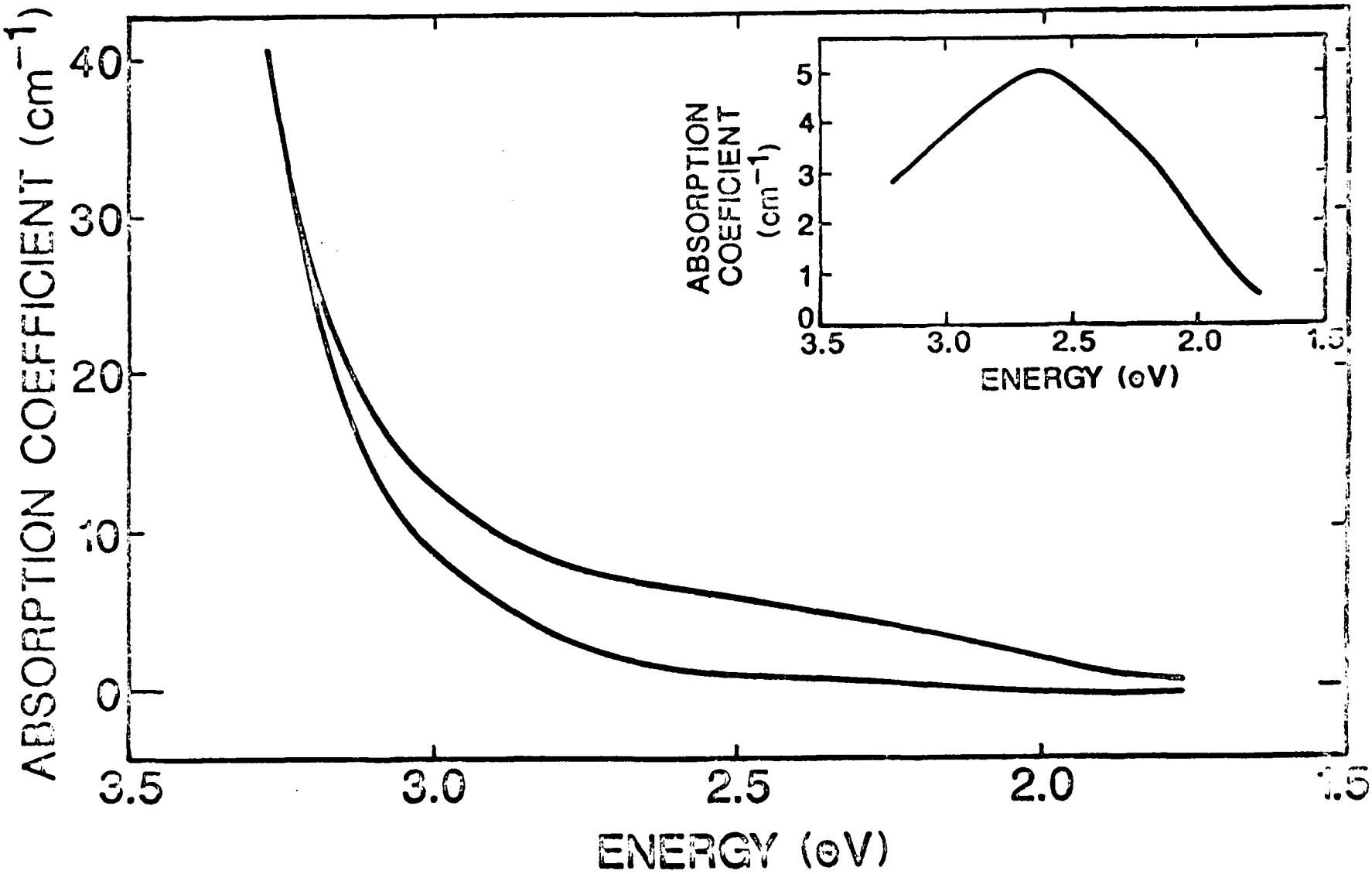
ABSORPTION COEFFICIENT (cm^{-1})
40
30
20
10
0
3.5
3.0
2.5
2.0
ENERGY (eV)
ABSORPTION COEFICIENT (cm^{-1})
5
4
3
2
1
0
3.5
3.0
2.5
2.0
ENERGY (eV)

END

DATE

FILMED

8-88

DTIC